A hyperthermal energy ion beamline for probing hot electron chemistry at surfaces

M. P. Ray, R. E. Lake, S. A. Moody, V. Magadala, and C. E. Sosolik
Department of Physics and Astronomy, Clemson University, Clemson, South Carolina 29634, USA

(Received 2 May 2008; accepted 24 June 2008; published online 25 July 2008)

An ultrahigh vacuum ion beamline and chamber have been assembled to produce hyperthermal (<400 eV) energy ions for studying hot electron chemistry at surfaces. The specific design requirements for this modified instrument were chosen to enable the exposure of a metal-oxide-semiconductor (MOS) device to monoenergtic, well-collimated beams of alkali ions while monitoring both the scattered beam flux and the device characteristics. Our goal is to explore the role that hot electrons injected toward the MOS device surface play in the neutralization of scattered ions. To illustrate the functionality of our system, we present energy-resolved spectra for Na^+, K^+, and Cs^+ ions scattered from the surface of a Ag(001) single crystal for a range of incident energies. In addition, we show MOS device current-voltage characteristics measured *in situ* in a new rapid-turnaround load lock and sample translation stage. © *2008 American Institute of Physics.*
[DOI: 10.1063/1.2960559]

The use of hyperthermal energy ion beams (1–400 eV) as probes of energy and charge transfer at surfaces has historically been quite limited due to the difficulties in creating and transporting adequate flux to a target in this energy regime.[1–5] This is in contrast to the use of low energy ions (0.4–20 keV) at surfaces, which are a common and easily accessible spectroscopic tool.[6] With the recent discovery of hot electron or chemicurrent-based pathways for energy loss at thin metal film surfaces,[7,8] there is a need for dedicated instruments that can produce hyperthermal energy beams and explore these phenomena in more detail. Here we describe a novel, ultrahigh vacuum ion scattering system that has been redesigned for rapid turnaround and *in situ* characterization of thin film metal devices under hyperthermal energy beam exposures.

The system is differentially pumped and divided into three sections that can be isolated using the all-metal inline valves shown in Fig. 1. The three sections are connected by flexible bellows that provide pumping impedances and allow for reasonably independent operating pressures in each section. The two primary beamline sections (I and II, separated by inline valve 1) are pumped using a turbomolecular pump (280 l/s) and an ion pump (30 l/s), respectively. The scattering chamber (Sec. III, separated by inline valve 2) is pumped by a combination of a turbomolecular pump (550 l/s), an ion pump (440 l/s), and a titanium sublimation pump.

Section I consists primarily of a Colutron G-2 ion gun[9] and a homebuilt ion source[10] that incorporates a commercially available alkali-doped aluminosilicate ion emitter[11] to produce singly charged alkali ions. All ions are transported to the scattering chamber at energies of 400 eV or higher to reduce space-charge spreading and the loss of beam flux. Since final kinetic energies less than 400 eV are desired at the sample position in Sec. III, the entire beamline (Secs. I and II) is placed at a negative voltage ($-400 < V_{float} < 0$ V) with respect to the ground potential of Sec. III.[12]

The flux of ions emerging from the aluminosilicate emitter is focused and mass selected into a Faraday cup mounted between Secs. I and II using an Einzel lens and Wien filter mounted within the ion gun housing. Symmetric sets of Einzel lenses and *X-Y* deflectors mounted at the entrance and exit apertures of a 90° spherical monochromator then transport the beam through Sec. II. The primary purpose of this section is to define the energy resolution of the ion beam at $\Delta E/E \sim 0.01$.[13] The energy-resolved flux passing through the monochromator is monitored at a second Faraday cup between Secs. II and III. Two Einzel lenses and a final set of *X-Y* deflectors focus the beam through a 1 mm aperture and into a third Faraday cup at the center of the scattering chamber.

Section III is a two-tier vacuum chamber that houses various surface analysis tools, two scattered particle detectors, and a six-axis manipulator stage. The manipulator stage holds a Faraday cup and translates samples between the two chamber tiers to facilitate both beam exposures in the lower tier and surface analysis in the upper tier. Mounted in the upper tier are a sputter gun, Auger electron spectrometer (AES), Kelvin probe, and a low energy electron diffraction (LEED) system. The lower tier holds both an ion and a neutral particle detector (NPD) mounted in plane with the incident ion beam on a differentially pumped rotatable flange. The ion detector uses a 180° electrostatic analyzer (ESA) combined with a channel electron multiplier to detect ions with $\Delta E/E = 0.016$. Absolute ratios of the neutral to total flux in the scattered beam and velocity-resolved spectra are determined with the NPD using beam pulsing and standard time-of-flight techniques.[14]

A newly designed load-lock system was added to the scattering chamber to facilitate rapid-turnaround beam exposures and characterization measurements using *ex situ* fabricated MOS devices. The system, connected to the lower chamber tier, is isolated via a 4 in. gate valve and pumped using a 150 l/s turbomolecular pump. A 4 in. elbow and

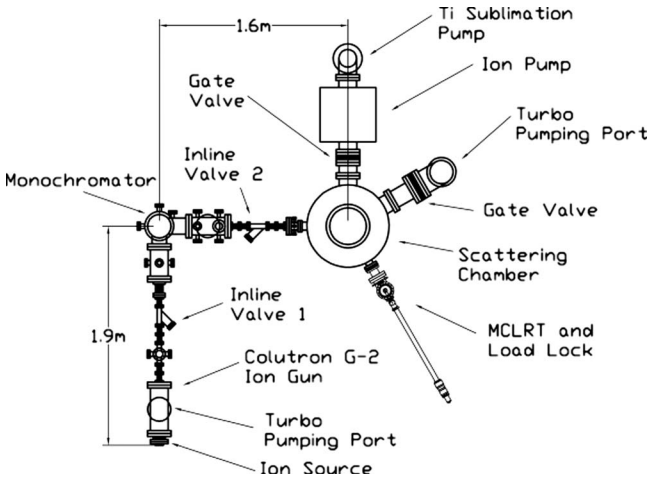

FIG. 1. A top-down schematic view of our UHV beamline. The two inline valves divide the system into three distinct sections. Two Faraday cups (not shown here) are mounted in the beam prior to each inline valve. A third Faraday cup is mounted at the center of the scattering chamber.

quick access door serve as the load-lock chamber which is connected to a magnetically coupled linear rotary transfer (MCLRT) rod with a 0.8 m stroke.[15] The MCLRT rod is used to place MOS devices directly in the ion beam path for exposures or to move sample transfer stages onto the manipulator of Sec. III. Our homebuilt transfer stages provide a flexible method for electrically contacting samples, heater filaments, and thermocouples. Moreover, they can be quickly modified or repaired *ex situ* depending on the mounting schemes required for MOS or other devices. A standard transfer stage, shown in Fig. 2, includes three locking rings and a faceplate separated by Macor® insulators. Each locking ring has two separate, electrically isolated halves, giving six total electrical contacts for use with a faceplate-mounted sample. Our typical mounting scheme also includes a coiled W filament placed directly behind the sample for both radiative and electron beam heating. The filament is placed in a Ta shield exposing only the back side of the sample to the heater. The shield protects components from electrical shorting due to metal deposition from the filament. A type K

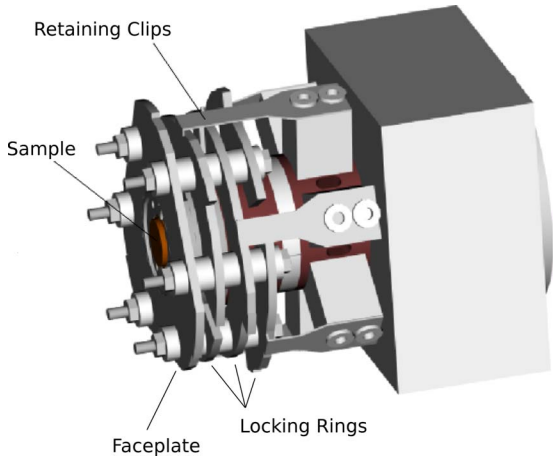

FIG. 2. (Color online) A rendering of the sample exchange system. A heater filament and thermocouple are located behind the sample. An extractor (not shown) is used to rotate the sample stage and disengage the retaining clips for removal from vacuum.

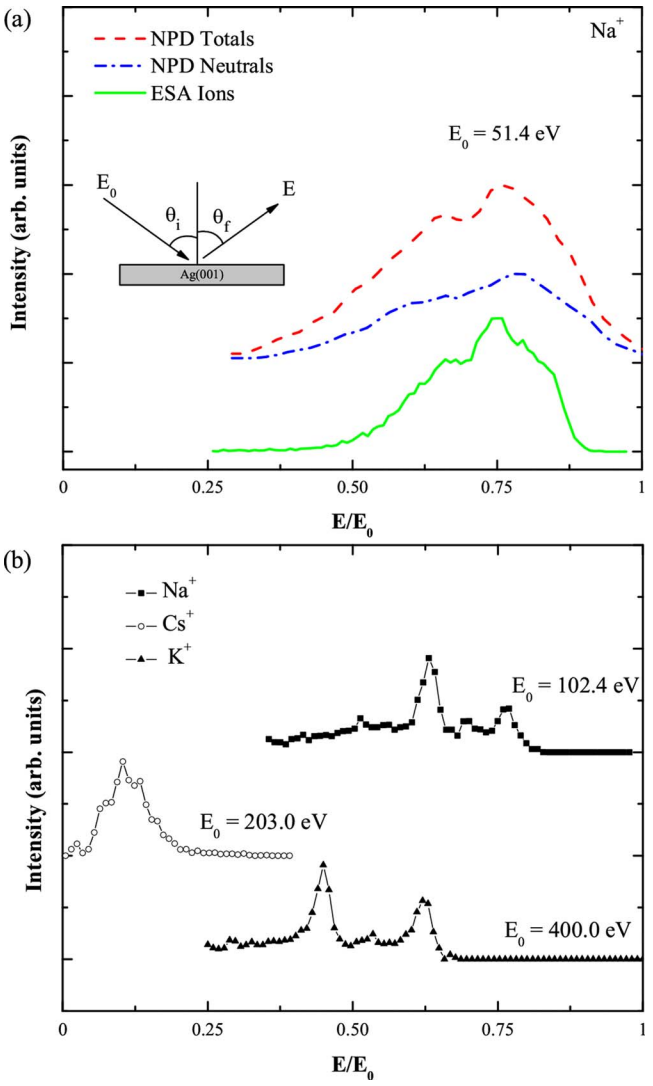

FIG. 3. (Color online) (a) NPD and ESA scattered spectra for a Na^+ ion beam incident on Ag(001) with $\theta_i = \theta_f = 55°$. The NPD total and neutral spectra are shifted up and rescaled for comparison with the ion-only ESA spectrum. The inset shows the scattering geometry for all spectra. (b) Representative ESA spectra for Na^+, K^+, and Cs^+ ions scattered from Ag(001) with $\theta_i = \theta_f = 45°$. For all spectra the ion beam was directed along the ⟨110⟩ crystal azimuth.

alumel-chromel thermocouple is mounted on or near the sample to monitor temperature. An extractor (not shown) can be attached to the MCLRT to remove the sample stage. It engages with the faceplate to rotate the full assembly and disengage the locking rings from the retaining clips. The clips serve as mechanical and electrical contacts to the manipulator.

In order to verify the operational parameters of the beamline, Na^+, K^+, and Cs^+ ions were scattered from a single crystal Ag(001) target along the ⟨110⟩ azimuth at various incident energies. The scattering azimuth was verified with a combination of LEED and ion scattering spectroscopy. The sample was cleaned using a sputter-annealing cycle consisting of a 500 eV Ar^+ sputter and an annealing at 420 °C. The sample was exposed to the alkali ion beam with scattered particles detected with the ESA and NPD. Sample cleanliness was verified using the AES. Figure 3(a) shows an ESA spectrum and NPD spectra for a Na^+ beam incident at

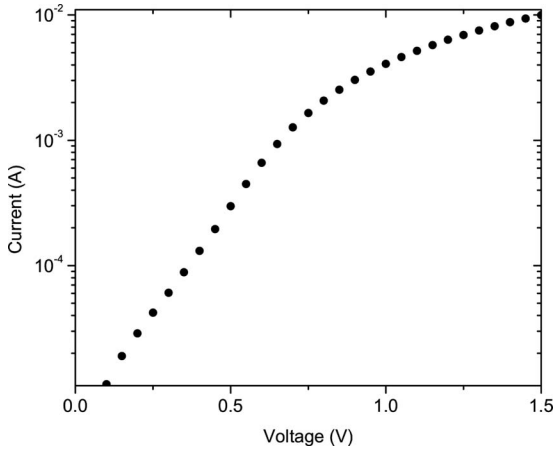

FIG. 4. An *I-V* measurement taken on a MOS device *in situ*. The device consists of a 7 nm thick Au layer on a 1 nm Ti wetting layer separated from the *n*-type Si substrate by 5 nm of SiO_2.

51.4 eV. Figure 3(b) shows only ESA spectra measured for three alkali species at incident energies between 100 and 400 eV. For the ESA spectra, the ion count obtained at each pass energy (E) has been multiplied by $1/E$ to account for the ESA transmission function. The Na^+ and K^+ spectra show multiple energy-resolved peaks that are consistent with sequential binary collisions between the ions and single surface atoms.[16] The Cs^+ spectrum shows a lower energy feature that is the result of the complex dynamics involved in a heavy atom-surface collision.[17]

The data in Fig. 4 demonstrate the functionality of the sample stage mounted on the MCLRT rod for *in situ* current-voltage (*I-V*) characterization of MOS devices. The measurement exhibits a high leakage current, however, the data verify the functionality of the sample stage for *in situ I-V* measurements. The *I-V* curve shown was taken on a Au/Si MOS device that consisted of a 7 nm Au layer on top of a 1 nm Ti wetting layer. The metal layers were separated from the *n*-doped Si substrate by a 5 nm SiO_2 layer. For this particular measurement, the device was mounted in a sample stage that placed it at 45° relative to the incident ion beam path. This unique arrangement allows us to obtain the device *I-V* characteristics while simultaneously measuring scattered ions or neutral particles. Our complete hyperthermal energy beamline coupled with this sample stage design will facilitate new investigations into charge transfer dynamics. For example, we will test the theoretical prediction that ballistically transported electrons passing through a MOS device can drive chemical processes at surfaces.[18,19]

This work was supported by the National Science Foundation (No. NSF-CHE-0548111). We also acknowledge assistance from Dr. Ib Chorkendorff and his research group at the Technical University of Denmark.

[1] D. L. Adler and B. H. Cooper, Rev. Sci. Instrum. **59**, 137 (1988).
[2] D. L. Adler, B. H. Cooper, and D. R. Peale, J. Vac. Sci. Technol. A **6**, 804 (1988).
[3] R. L. McEachern, D. L. Adler, D. M. Goodstein, G. A. Kimmel, B. R. Litt, D. R. Peale, and B. H. Cooper, Rev. Sci. Instrum. **59**, 2560 (1988).
[4] A. D. Tenner, K. T. Gillen, T. C. M. Horn, J. Los, and A. W. Kleyn, Surf. Sci. **172**, 90 (1986).
[5] E. Hulpke and K. Mann, Surf. Sci. **133**, 171 (1983).
[6] J. W. Rabalais, *Principles and Applications of Ion Scattering Spectrometry: Surface Chemical and Structural Analysis* (Wiley, Hoboken, NJ, 2003), Chap. 1, and references therein.
[7] H. Nienhaus, H. S. Bergh, B. Gergen, A. Majumdar, W. H. Weinberg, and E. W. McFarland, Phys. Rev. Lett. **82**, 446 (1999).
[8] B. Gergen, H. Nienhaus, W. H. Weinberg, and E. W. McFarland, Science **294**, 2521 (2001).
[9] Colutron Research Corporation, Boulder, CO.
[10] D. R. Peale, D. L. Adler, B. R. Litt, and B. H. Cooper, Rev. Sci. Instrum. **60**, 730 (1989).
[11] HeatWave Labs, Inc., Watsonville, CA.
[12] The beamline can also be used without a floating voltage to run beams with kinetic energies up to 10 keV.
[13] The monochromator also blocks the propagation of energetic neutral particles and photons down the beamline.
[14] G. A. Kimmel and B. H. Cooper, Rev. Sci. Instrum. **64**, 672 (1993).
[15] Thermionics Vacuum Products, Port Townsend, WA.
[16] C. A. DiRubio, R. L. McEachern, J. G. McLean, and B. H. Cooper, Phys. Rev. B **54**, 8862 (1996).
[17] C. E. Sosolik and B. H. Cooper, Nucl. Instrum. Methods Phys. Res. B **182**, 167 (2001).
[18] J. W. Gadzuk, Phys. Rev. Lett. **76**, 4234 (1996).
[19] J. W. Gadzuk, J. Vac. Sci. Technol. A **15**, 1520 (1997).